

Document downloaded from:

<http://hdl.handle.net/10251/103141>

This paper must be cited as:

Benítez-González, J.; Mora Almerich, J. (2017). Sensitivity Enhancement for Low-Coherence Interferometry. *IEEE Photonics Technology Letters*. 29(20):1735-1738. doi:10.1109/LPT.2017.2748818



The final publication is available at

<https://doi.org/10.1109/LPT.2017.2748818>

Copyright Institute of Electrical and Electronics Engineers

Additional Information

Sensitivity enhancement for low coherence interferometry

J. Benítez, J. Mora

Abstract— In this letter, a sensitivity improvement for systems combining low coherence interferometry (LCI) and microwave photonics (MWP) is demonstrated. This improvement is due to the introduction of a different modulation format and an exhaustive control of the optical source profile compared to previous MWP-LCI schemes. Our proposal allows to retrieve the visibility of low-coherence interferograms through the analysis of the interference pattern using a dispersive element. We demonstrate that the use of a phase modulator offers better stability and lower insertion loss since a bias point configuration is not needed compared to the intensity modulators typically used in these schemes. The process for controlling the optical source profile permits a comparison between uniform and gaussian profiles. In this way, the limiting effects of the sidelobes over the achieved sensitivity level are analyzed. The proposed MWP-LCI structure is experimentally demonstrated through the characterization of the electrical transfer function. In this case, a maximum sensitivity of 65 dB is achieved in our MWP-LCI structure showing a 30 dB improvement compared to current proposals.

Index Terms— Low coherence interferometry, microwave photonics, optical profile, phase modulation, sensitivity.

I. INTRODUCTION

LOW coherence interferometry (LCI) is an extended measurement technique able to give excellent precision in the axial direction. An incoherent source is employed to illuminate a sample and a reference surface such as a mirror. The combination of the backscattered light coming from the sample and the reflection in the mirror surface creates an interference pattern, whose analysis can determine the position of the events produced in the axial direction of a sample [1]. Currently, the main field of application in LCI is medicine through the optical coherence tomography (OCT) [2]. LCI is also interesting in applications such as components characterization [3] or physical magnitude sensing [4].

Although LCI is a widely employed technique, the current solutions show a lack of stability and cost effectiveness what implies an increment in the design complexity. Current proposals are focused in improving the key parameters of LCI

as sensitivity, penetration depth or resolution. In this context, the combination of LCI and Microwave Photonics (MWP) permits to solve these issues by exploiting the inherent stability of the interference pattern in the RF domain. For instance, a method for retrieving low-coherence interferograms was proposed by slicing an incoherent optical source and analyzing it employing a dispersive element [5]. Besides, in [6] a single side-band modulation approach is employed in order to improve the total measurable range of the current MWP-LCI schemes. Despite both proposals demonstrate the feasibility of this technique; the current key parameters of the MWP-LCI proposals are limited, especially in terms of sensitivity. In this sense, it is necessary to explore new solutions to this issue.

In current MWP-LCI configurations [5,6], intensity modulation (IM) is employed as the typical modulation format in commercial applications. As known, an intrinsic optical loss in the modulation process is produced due to the biasing polarization. Moreover, the existence of a bias drift is also common in this process mainly due to the combination of pyroelectric, photorefractive and photoconductive effects concerning the electro-optic materials [7]. In this sense, we propose to analyze alternative modulation formats to achieve an improvement on the key parameter of the MWP-LCI systems. Concretely, the use of phase modulation (PM) can be a feasible solution in order to reduce optical losses in a MWP-LCI structure as there is no need of biasing the modulator.

In this context, a MWP-LCI scheme is proposed by means of PM-IM conversion through a dispersive element with an additional control of the optical power spectrum density in order to improve sensitivity compared to previous approaches. In order to analyze the obtained improvement compared to previous proposals [5,6], theoretical and experimental analyses are carried out. Moreover, we attach a study where the importance of the control in the optical source profile is shown in order to improve the sensitivity level. For the proposed MWP-LCI structure, a maximum sensitivity value of 65 dB with a resolution value of 120 μm is achieved.

II. SYSTEM DESCRIPTION

The layout of the proposed MWP-LCI structure is shown in Fig.1. The main target of this work is focused on the sensitivity improvement compared to previous approaches [5,6]. For this, we propose a scheme with phase modulation (PM) as a novel modulation format for MWP-LCI and a complete control of the optical power spectrum density. In this

Manuscript received January 19th, 2017. The research leading to these results has received funding from the National Project TEC2014-60378-C2-1-R funded by the Ministerio de Ciencia y Tecnología and the regional project PROMETEO FASE II/2013/012 funded by the Generalitat Valenciana.

The authors are with the ITEAM Research Institute, Universitat Politècnica de València, Valencia, Spain (e-mail: jmalmer@iteam.upv.es).

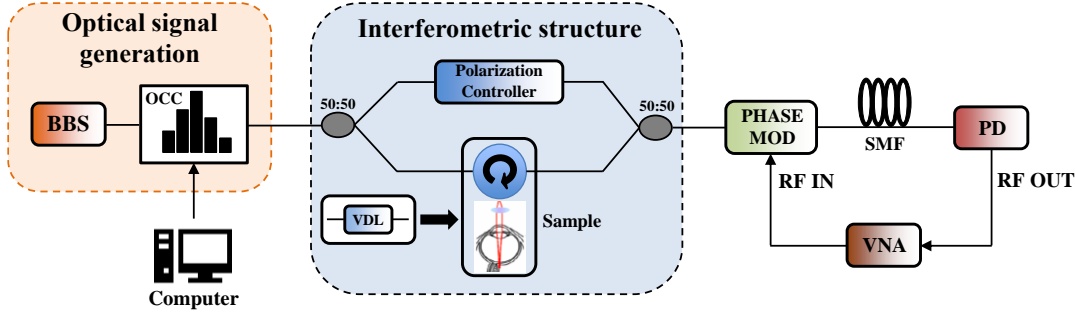


Fig. 1. Layout of the proposed MWP-LCI with phase modulation and control of the optical source power profile.

structure, a broadband source (BBS) and an optical channel controller (OCC) are set to generate the desired optical power profiles. The BBS has a total bandwidth of 80 nm and the OCC (WaveShaper 4000S) is centered in 1547.22 nm and has 5026 independent channels separated 8 pm. Each channel can be attenuated independently with a potential range of 50 dB. The control of the optical profile is externally performed by a personal computer. Then, the optical signal generated is introduced in a Mach-Zehnder interferometer (MZI) by means of a 50:50 optical coupler. In the upper arm, a polarization controller device is placed in order to control the polarization state inside the interferometric structure. This control also ensures the maximum visibility of the interference. In the lower arm, the sample under test would be placed by means of an optical circulator. For simplicity, a variable delay line (VDL) is employed in order to emulate the behaviour of a real sample. The optical path difference (OPD) produced between both arms is the origin of the slicing of the optical source signal which period is proportional to the OPD in the interferometer. After the interferometric structure a phase modulator is placed in the structure (PHASE MOD). This device performs the electro-optic conversion of the optical signal. The RF signal employed in this process is generated by a vector network analyzer (VNA) (Agilent E8364A) labeled in Fig. 1 as RF IN. In Eq. (1), the signal $m(t)$ describes the type of modulation performed:

$$m(t) = \sum_k a_k \cdot e^{jk\Omega t} \quad a_{k,PM} = \sqrt{\alpha_{PM}} \cdot J_k(m/2) \quad (1)$$

where the non-linear terms a_k for a phase modulator are given by the insertion loss α_{PM} , the modulation index m and the Bessel function J_k of the first kind and order k [8].

The modulated signal is then launched into a dispersive element with an accumulated dispersion of $\ddot{\varphi}_2 = -227 \text{ ps}^2$, i.e., a 10 km single mode fiber (SMF). PM-IM conversion can be easily performed by a dispersive device as a SMF [9]. Finally, for the detection stage, a single photodetection is performed (PD). In this case, the RF signal obtained after the PD (RF OUT) is the signal that contains the information of the OPD introduced by the sample. By taking this signal to the VNA, the electrical transfer function of the system can be analyzed through the obtention of the S21 parameter.

The MWP-LCI structure proposed in Fig. 1 can be theoretically described by generalizing the development made in [10]. Following a similar procedure, our MWP-LCI

proposal can be theoretically described by generalizing this previous development. Concretely, we define the electrical transfer function of the structure H_{OUT} for any modulation format considering a small signal approach with a generic n -layered sample scenario:

$$H_{OUT}(\Omega) = H_{MOD}(\Omega) \cdot H_{LCI}(\Omega) \quad (2)$$

From (2), we can differentiate two main contributions. The first term H_{MOD} is determined by the effects of the modulation process and the dispersive element:

$$H_{MOD}(\Omega) \approx \left[a_0 a_{-1}^* \cdot e^{j\frac{1}{2}\ddot{\varphi}_2 \Omega^2} + a_1 a_0^* \cdot e^{-j\frac{1}{2}\ddot{\varphi}_2 \Omega^2} \right] \quad (3)$$

The second term corresponding to Eq. (2) is related to the LCI response (H_{LCI}) where H_n and τ_n represent the corresponding reflectivity and the delay associated to the n -layer of the sample, respectively. The term R_M is the reflectivity related to the upper arm of the interferometer.

$$\begin{aligned} H_{LCI}(\Omega) \approx & \sum_n \underbrace{\left(|H_n|^2 \cdot e^{-j\Omega\tau_n} + |R_M|^2 \right)}_{DC} \cdot \tilde{S}(\Omega) - \\ & \underbrace{-H_n \cdot R_M^* \cdot e^{-j\Omega\tau_n/2}}_{+\Omega_n} \cdot \tilde{S}(\Omega - \Omega_n) - \\ & \underbrace{-H_n^* \cdot R_M \cdot e^{-j\Omega\tau_n/2}}_{-\Omega_n} \cdot \tilde{S}(\Omega + \Omega_n) \end{aligned} \quad (4)$$

From (4), a DC component and several RF resonances around the electrical frequency $\pm\Omega_n$ can be distinguished. The central frequency of these RF resonances is closely related to the OPD_n related to each n -th-layer, i.e.:

$$\Omega_n = -\frac{2 \cdot OPD_n}{c_0 \cdot \ddot{\varphi}_2} \quad (5)$$

where c_0 is the speed of light in vacuum. Note that each contribution in (4) is given by the term $\tilde{S}(\Omega)$ which represents the Fourier transform of the optical source in the following form:

$$\tilde{S}(\Omega) = \frac{1}{2\pi} \int_{-\infty}^{\infty} S(\omega) \cdot e^{-j\ddot{\varphi}_2 \Omega \omega} d\omega \quad (6)$$

In order to show the performance of the proposed MWP-LCI structure, we consider a VDL as a single sample set two different OPDs. First of all, the PM-IM conversion must be performed in order to recover the RF signal using a PD. This fact can be seen in the sinusoidal term H_{MOD} of the following expression introducing (1) into (2):

$$H_{MOD}^{PM}(\Omega) \approx \left[-2j \cdot \alpha_{PM} \sin\left(\frac{\dot{\phi}_2 \Omega^2}{2}\right) J_0\left(\frac{m}{2}\right) J_1\left(\frac{m}{2}\right) \right] \quad (7)$$

In Fig. 2, the PM-IM conversion is plotted using a tunable laser to describe (7). Taking into account the experimental parameters, a useful window around 15 GHz is obtained.

In order to show the properties of the term H_{LCI} , two samples are considered with an OPD set to 2.78 mm and 3.64 mm for different optical sources profiles. Concretely, uniform and gaussian profiles with a 3dB bandwidth of 8.8 and 6.4 nm, respectively, are achieved through the optical source generation stage for the experimental measurement. We can observe that for each profile, an RF resonance is generated around 13 and 17 GHz, for the gaussian and uniform profiles, respectively, as predicted by (5). In this case, the resolution of the MWP-LCI proposed system is obtained from Fig. 2 with a similar value around 120 μm for both profiles.

Fig. 2 shows that experimental results for both profiles are free from the baseband component that the theoretical analysis predicts according to (4). In this way, the PM-IM conversion improves the global response of the electrical response since it has a lowpass characteristic as shown in (7). Indeed, one of the main contributions of noise is produced by the baseband component and its sidelobes.

III. SENSITIVITY ANALYSIS

Sensitivity is one of the most important parameters in LCI-based systems. In OCT applications, sensitivity is generally defined as the lower reflectivity coming from the sample that can be detected by the system. Numerically, it is usually related to a signal-to-noise ratio (SNR) value of $\text{SNR}=1$ [11]. Consequently, in order to improve sensitivity compared to previous MWP-LCI approaches [5,6], two different scenarios are considered: increasing the total signal level or reducing the noise contribution.

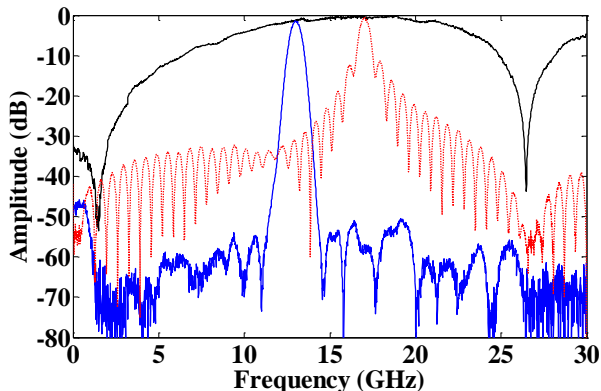


Fig. 2. Electrical transfer function for uniform (—) and gaussian (---) profiles versus the frequency. PM-IM conversion is added in continuous black line.

The optimization of the structure in terms of optical losses is an excellent step in order to increase the final signal level. Furthermore, noise contribution is practically originated by the baseband component and its sidelobes in this kind of systems as abovementioned. In this sense, the configuration of the optical power profile is critical for the control of the noise generated by the structure. In this context, we propose a sensitivity analysis focuses on two points. Firstly, a comparison between our structure and the modulation format used in previous approaches. Secondly, an analysis of different optical power profiles in order to examine its importance over the sensitivity.

A. Modulation format (analysis of H_{MOD})

In order to demonstrate that the use of PM format is beneficial for improving sensitivity, we need to compare the effects of IM and PM in the term H_{MOD} . Therefore, we first need to particularize (3) for IM using:

$$a_{n,IM} = \sqrt{\alpha_{IM}} \cdot B_n \cdot J_n(m/2) \quad (8)$$

where α_{IM} represents the insertion loss of the intensity modulator and B_n is the term related to the bias configuration.

By taking (8) into account, we can find the corresponding transfer function for IM operating in quadrature:

$$H_{MOD}^{IM}(\Omega) \approx \left[-j \cdot \alpha_{IM} \cos\left(\frac{\dot{\phi}_2 \Omega^2}{2}\right) J_0\left(\frac{m}{2}\right) J_1\left(\frac{m}{2}\right) \right] \quad (9)$$

A direct comparison can be then established between the electrical response of (7) and (9). The most important difference is found in the factor 2 and the insertion losses. This factor is caused by the need of setting the bias configuration of the intensity modulator to its quadrature point. This fact involves an intrinsic minimum loss of 6 dB of IM compared to PM in the experimental measurements. Moreover, the employment of a different modulator implies a different value in the insertion loss (α_{AM} and α_{PM}) that can slightly affect the output RF signal level. However, this fact is not controllable since it depends on the manufacturer and it is not a solid point of comparison. Finally, we observe that the term related to the dispersive element is different in (7) and (9). For IM case as shown in (9), CSE is the main limitation since the RF resonance is removed for certain electric frequencies. In LCI systems this involves a limited penetration depth. However, for PM an additional benefit is produced due to the notch near to DC as shown in Fig. 2.

B. Optical source power profile control (analysis of H_{LCI})

In MWP-LCI systems, the electrical transfer function obtained when the sample is not present in the interferometer ($H_n = 0$) is considered as the noise contribution and it permits to calculate sensitivity of the system.

In order to analyze the relationship between the optical power profile and the noise contribution, Fig. 3 shows the electrical noise response for the uniform and gaussian profiles used for Fig. 2. A similar normalization procedure has been applied in this case as in Fig. 2. We observe that the electrical

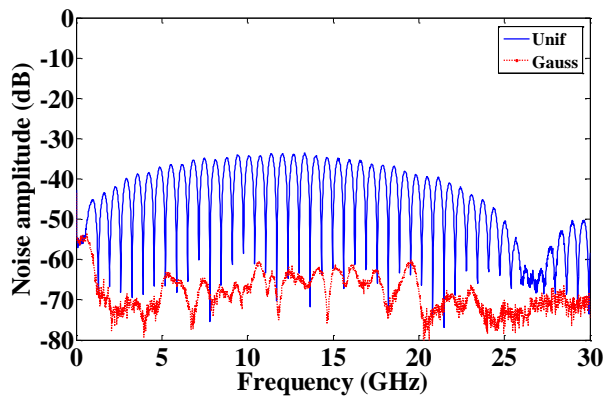


Fig. 3. Electrical transfer function of the noise contribution when a uniform (—) and a gaussian (---) are employed as optical source power profiles.

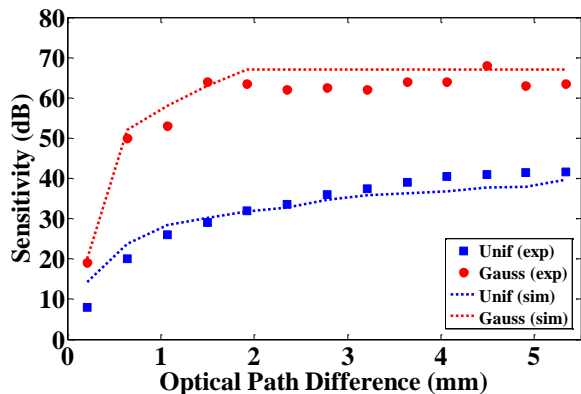


Fig. 4. Sensitivity for uniform (■) and gaussian (●) profiles versus OPD. Simulations of the sensitivity are added in dashed line for each profile.

noise contribution sidelobes for the uniform profile are much higher compared to the gaussian profile although the optical power level of the integrated signal is similar.

Therefore, the residual signal present in this electrical transfer function is originated by the sidelobes of the baseband component. From (6), we can observe that the shape of the RF resonance can be identify as an inverse Fourier transform (IFT) of the original optical source profile scaled to the electrical frequency. Therefore, the electrical of the baseband contribution is mainly determined by the selected profile at the optical signal generation stage.

Finally, a comparison between the sensitivity achieved by the uniform and gaussian profiles is attached. For this, the amplitude of the RF resonance originated when different OPDs are set in the interferometer has been measured. In order to obtain the sensitivity of each profile, the noise contributions seen in Fig. 3 have been considered. Results obtained are depicted in Fig. 4. We can observe that for the uniform profile, the sensitivity obtained is clearly affected by the PM-IM conversion for low OPDs which corresponds with RF frequencies close to baseband. For that case, a maximum sensitivity of 40 dB is achieved. However, for the gaussian profile an important difference compared to the uniform profile is found since the sidelobes are much lower in all the range measured as depicted in Fig. 3. In this case, a maximum sensitivity of 65 dB has been obtained, demonstrating that the control of the optical source power profile can considerably

improve sensitivity level. Compared to previous proposals [5,6], a 30 dB improvement has been achieved in our work. Theoretical simulations of the sensitivity have been added in dashed line showing the good agreement with the experimental results for both profiles.

IV. CONCLUSION

In this letter, a MWP-LCI structure combining phase modulation and a complete control of the optical signal profile is proposed in order to improve sensitivity achieved compared to previous proposals [5,6]. A theoretical description of the structure is addressed where we conclude that the use of intensity modulators is a drawback in terms of sensitivity compared to the phase modulator due to the biasing polarization. Furthermore, the relevance of the optical signal profile in obtaining sensitivity is also presented. We have observed that the noise contribution of the structure is produced by the baseband component. In this case, the comparison in terms of sensitivity of a uniform and a gaussian profile is provided. We have demonstrated that the sidelobes of each profile implies an extremely different value for the achieved sensitivity level. In this way, a 30 dB improvement for sensitivity has been obtained compared to previous proposals using phase modulation and a gaussian profile with a maximum sensitivity level of 65 dB.

REFERENCES

- [1] J. Pluciński, R. Hyszer, P. Wierzba, M. Strąkowski, M. Jędrzejewska-Szczerska, M. Maciejewski and B.B. Kosmowski, "Optical low-coherence interferometry for selected technical applications," *Bull. Pol. Acad. Sci., Tech. Sci.*, vol. 56, no. 2, pp. 155-172, 2008.
- [2] D. Huang, E. A. Swanson, C. P. Lin, J. S. Schuman, W. G. Stinson, W. Chang, M. R. Hee, T. Flotte, K. Gregory and C. A. Puliafito, "Optical Coherence Tomography," *Science*, vol. 254, pp. 1178-1181, Nov. 1991.
- [3] P. Nandi, Z. Chen, A. Witkowska, W. J. Wadsworth, T. A. Birks and J. C. Knight, "Characterization of a photonic crystal fiber mode converter using low coherence interferometry," *Opt. Lett.* vol. 34, no. 7, pp. 1123-1125, 2009.
- [4] P.V. Volkov, A.V. Goryunov, A.Yu. Luk'yanov, A.D. Tertyshnik, N.A. Baidakova and I.A. Luk'yanov, "Fiber-optic temperature sensor based on low-coherence interferometry without scanning," *Optik*, vol. 124, no. 15, pp. 1982-1985, 2013.
- [5] C. R. Fernandez-Pousa, J. Mora, H. Maestre and P. Corral, "Radio-frequency low-coherence interferometry," *Opt. Lett.*, vol. 39, no. 12, pp. 3634-3637, Jun. 2014.
- [6] J. Benítez, M. Bolea and J. Mora, "High-performance low coherence interferometry using SSB modulation", *IEEE Photon. Technol. Lett.* 29(1), 90-93 (2017)
- [7] J. Švarný, "Analysis of quadrature bias-point drift of Mach-Zehnder electro-optic modulator," in *12th Biennial Baltic Electronics Conference*, Tallinn, 2010, pp. 231-234.
- [8] I. Gasulla and J. Capmany, "Analytical model and figures of merit for filtered Microwave photonic links," *Opt. Express*, vol. 19, no. 20, pp. 19758-19774, 2011.
- [9] H. Chi, X. Zou, and J. Yao, "Analytical Models for Phase-Modulation-Based Microwave Photonic Systems With Phase Modulation to Intensity Modulation Conversion Using a Dispersive Device," *J. Lightwave Technol.*, vol. 27, no. 5, pp. 511-521 (2009).
- [10] J. Mora, B. Ortega, A. Díez, J. L. Cruz, M. V. Andrés, J. Capmany, and D. Pastor, "Photonic Microwave Tunable Single-Bandpass Filter Based on a Mach-Zehnder Interferometer," *J. Lightw. Technol.*, vol. 24, no. 7, pp. 2500-2509, 2006.
- [11] M. Wojtkowski, "High-speed optical coherence tomography: basics and applications," *Appl. Opt.*, vol. 49, no. 16, pp. D30-D61, 2010.